

Zeitschrift: IABSE reports = Rapports AIPC = IVBH Berichte

Band: 62 (1991)

Artikel: Load carrying mechanism of anchor bolt

Autor: Maruyama, Kyuichi / Shimizu, Keiji / Momose, Mitsuhiro

DOI: <https://doi.org/10.5169/seals-47712>

Nutzungsbedingungen

Die ETH-Bibliothek ist die Anbieterin der digitalisierten Zeitschriften auf E-Periodica. Sie besitzt keine Urheberrechte an den Zeitschriften und ist nicht verantwortlich für deren Inhalte. Die Rechte liegen in der Regel bei den Herausgebern beziehungsweise den externen Rechteinhabern. Das Veröffentlichen von Bildern in Print- und Online-Publikationen sowie auf Social Media-Kanälen oder Webseiten ist nur mit vorheriger Genehmigung der Rechteinhaber erlaubt. [Mehr erfahren](#)

Conditions d'utilisation

L'ETH Library est le fournisseur des revues numérisées. Elle ne détient aucun droit d'auteur sur les revues et n'est pas responsable de leur contenu. En règle générale, les droits sont détenus par les éditeurs ou les détenteurs de droits externes. La reproduction d'images dans des publications imprimées ou en ligne ainsi que sur des canaux de médias sociaux ou des sites web n'est autorisée qu'avec l'accord préalable des détenteurs des droits. [En savoir plus](#)

Terms of use

The ETH Library is the provider of the digitised journals. It does not own any copyrights to the journals and is not responsible for their content. The rights usually lie with the publishers or the external rights holders. Publishing images in print and online publications, as well as on social media channels or websites, is only permitted with the prior consent of the rights holders. [Find out more](#)

Download PDF: 17.01.2026

ETH-Bibliothek Zürich, E-Periodica, <https://www.e-periodica.ch>

Load Carrying Mechanism of Anchor Bolt

Résistance d'un boulon d'ancrage chargé

Tragfähigkeit von Ankerbolzen

Kyuichi MARUYAMA

Assoc. Prof.
Nagaoka Univ. of Technology
Nagaoka, Japan

Kyuichi Maruyama, born 1948, received Ph.D. from the University of Texas at Austin in 1979. His research interests include durability of reinforced concrete structures.

Keiji SHIMIZU

Prof.
Nagaoka Univ. of Technology
Nagaoka, Japan

Keiji Shimizu, born 1928, received Doctor of Agriculture from the Univ. of Tokyo in 1971. He has extensive experience in railroad engineering.

Mitsuhiro MOMOSE

Civil Engineer
Nagano Pref. Office
Nagano, Japan

Mitsuhiro Momose, born 1966, received Master of Engineering from Nagaoka University of Technology in 1990.

SUMMARY

It is discussed in this paper how an anchor bolt, embedded in concrete, carries the applied load under static and fatigue loadings. An experimental test was conducted using anchor bolts of relatively small size in diameter and length. Examining the failure mode of concrete in detail, a mechanical model is developed in terms of an angle of crack propagation, stress distribution and the tensile strength of concrete.

RÉSUMÉ

Ce rapport décrit la façon dont un boulon d'ancrage dans le béton supporte l'application d'une charge statique et endure la fatigue. L'expérience a été menée sur des boulons d'ancrage relativement de petite taille (longueur et diamètre). Après observation du mode de rupture du béton environnant, un modèle mécanique est développé en fonction de l'angle de propagation de la fissure, de la distribution des contraintes et de la résistance du béton à la traction.

ZUSAMMENFASSUNG

In diesem Aufsatz wird erörtert, wie ein im Beton eingebetteter Ankerbolzen die Last unter statischen und ermüdenden Belastungen trägt. Der Versuch wurde mit in Durchmesser und Länge relativ kleinen Ankerbolzen durchgeführt. Nach sorgfältiger Prüfung des Betonbruchs wurde ein mechanisches Modell unter Berücksichtigung des Winkels des Rissfortschritts, der Verteilung der Spannung und der Zugfestigkeit des Betons entwickelt.



1. INTRODUCTION

The authors have reported the characteristics of the newly developed fixings (undercut type fixings) in terms of the static and fatigue strength, the applicability near the edge or the corner of concrete structures [1]. In the paper the empirical formulas were proposed for estimating the static and fatigue strength of such type fixings based on the experimental results. However, the formulas were limited to the fixings having 40 mm embedment length because of the limited range of test data. It was necessary to extend the study on the load carrying mechanism of the fixings from the low load level up to the failure stage with variations of embedment length and dimension of bolt.

In order to develop a general model of load carrying mechanism of the fixings, the static pull-out test was first conducted varying both the embedment length of bolt and the location of bolt from the edge of concrete block specimen. Referring to the study on application of acoustic emission to the pull-out test of anchor bolt [2], the discussion was extended to how the concrete carried the applied load, and what was the rational expression for the load carrying capacity of the undercut type fixings. The study should be applicable to the load carrying mechanism of ordinary anchor bolt because the load transfer point from the bolt to the surrounding concrete of this fixings is similar to that of ordinary anchor bolt.

2. EXPERIMENT

2.1 Bolts

The main parameters in the experiment were the size (diameter) and the embedment length of bolt. The shape of bolt is shown in Fig.1 and the dimension is summarized in Table 1. The tensile strength of bolt was 800 MPa. In order to assure the anchorage of bolt, the torque listed in Table 1 was applied to a bolt in advance of the pull-out test.

Concrete Block (cm)	Size of bolt (mm)	Torque (KN·cm)
	d le ϕ D	
50x50x20	14x40 M10 18	2.35
60x60x30	14x60 M10 18	3.53
	18x80 M12 24	6.76
120x60x30	22x100 M16 28	11.8

Table 1 Dimension of bolt

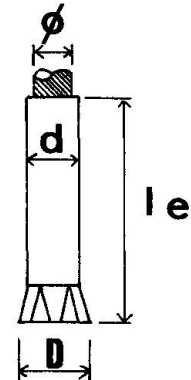


Fig.1 Shape of bolt

2.2 Test Setup

Fig.2 shows the test setup. The load was applied to a bolt by a center hole type oil jack, and was measured by a load cell of 50 KN or 200 KN capacity. The displacement was measured by LVDT's. In order to avoid the confinement effect due to the reaction supports, the supports were placed 3 times of embedment length (3·le) away from the bolt.

All the data were recorded and stored in a micro-computer through a dynamic strain meter and an A/D converter. The similar system was used for the fatigue test. The strength of concrete block specimen was evaluated by the compressive strength test using a cylindrical specimen of $\phi 10 \times 20$ cm.

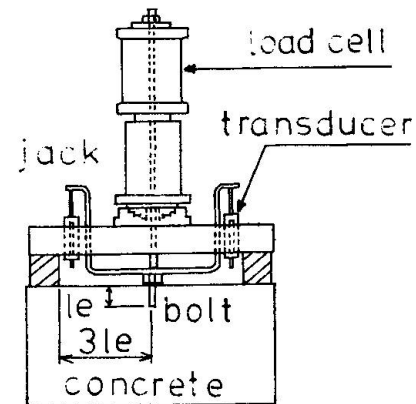


Fig.2 Test setup

3. TEST RESULTS AND DISCUSSION

After the pull-out test, the failure mode of the specimen was examined concerning with the shape of ruptured cone of concrete. A typical projection of cone is shown in Fig.3. The failure surface can be simplified as a tri-linear line as shown in Fig.4. Near the bottom end of bolt the concrete was splitted, and the crack developed at an angle of ϕ from the horizontal. At a certain point the angle of crack propagation turned to θ . Finally, the ruptured cone was pulled out with the skirt of shallow angle near the surface of concrete.

Since the measurement of cone depth was done in the four directions, Table 2 shows four values of ϕ and θ . The shallow angle of the skirt of cone was not shown because it was less important in the load carrying mechanism as will be discussed in the next section. The first angle (ϕ) ranged from 26 to 50 degree, and the second one (θ) from 20 to 40 degree. There observed little influence of the diameter and the embedment length of bolt, and of the concrete strength on the angles. The mean values were 39 and 27 degree for ϕ and θ , respectively. Some data of ϕ are not shown because too much rupture of concrete made the measurement of angle impossible. The location of turning point of the crack angle from ϕ to θ was observed scarcely influenced by the embedment length of bolt and the concrete strength. In the test it was about 1 cm away from the center of bolt (Fig.4). The examination was extended to the mortar block. The results were similar to those of concrete block, showing $\phi=36$ and $\theta=24$ degree.

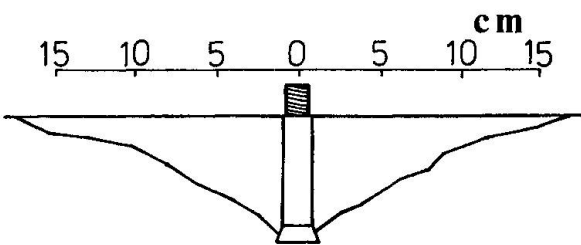


Fig.3 Ruptured cone

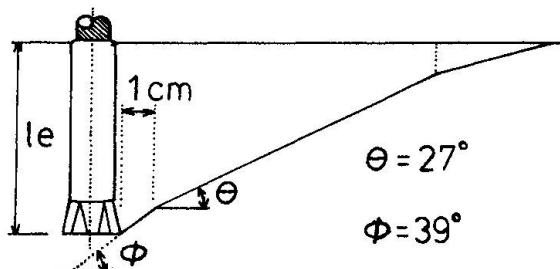


Fig.4 Simplified cone

Bolt d le ϕ	f_c MPa	f_t MPa	ϕ (degree)				θ (degree)				P_{max} KN
			41	34	48	--	28	20	48	25	
14x40 M10	19.2	1.75	36	43	27	--	24	30	27	27	20.8
14x60 M10	38.7	2.84	--	--	--	--	26	20	27	45	44.1
			47	42	46	--	29	27	27	25	55.0
			37	45	48	35	15	18	21	25	38.4
18x80 M12	31.4	2.24	45	38	--	--	30	30	25	30	61.9
	38.7	2.84	29	32	53	45	24	35	21	29	65.7
	37.3	2.52	49	41	--	--	21	26	23	22	55.0
22x100 M16	37.3	2.52	37	26	41	30	37	28	24	38	90.6
			35	30	36	--	30	30	31	16	86.2
			38	54	--	--	34	32	--	--	109
14x40 M10	37.4*	2.39	42	33	51	20	27	24	26	20	22.3
Mean Value			39.2				27.1				
Standard Deviation			8.2				6.5				
Coeff. of Variation			20.8 %				24.0 %				

* : Block was made of mortar.

Table 2 Test results



4. MODELLING OF LOAD CARRYING MECHANISM

Before constructing a mechanical model, the pertinent researches were surveyed. Rokugo et al [2] reported that up to the maximum load level the acoustic emission in the pull-out test generated within the circle area having the radius of 1.6 times of embedment length ($1.6 \cdot le$; Figs.5,6). On the other hand, the finite element analyses done by Kamimura [3] and Kosaka [4] showed that the principal tensile stress became to zero at the location of $(1.7-1.8) \cdot le$ away from the center of bolt. The similar results were obtained by the other series of test which examined how the pull-out resistance of anchor bolt was influenced by varying the bolt location from the edge of concrete block.

Taking these results into account, the load carrying mechanism of anchor bolt was modelled on the following assumptions (See Fig.7).

- (1) Crack initiates and propagates along the assumed cone line as shown in Fig.4.
- (2) At the tip of crack (distance of x from the bolt center in Fig.7), the applied load is resisted by both the splitting strength of uncracked portion of concrete (outside the tip of crack) and the frictional resistance of cracked portion (inside the tip of crack). The distribution of resistant stress is assumed to be an isosceles triangle.
- (3) Crack begins to propagate when the stress at the tip of crack exceeds the modulus of rupture of concrete (f_{tx}).
- (4) The modulus of rupture of concrete depends upon the confinement condition of concrete. As shown in Fig.7 the modulus of rupture near the bottom end of bolt is assumed to be 1.2 times of (f_t) which is given by the standard test [5]. The confinement effect decreases and fades out at the location of $1.7 \cdot le$ away from the center of bolt.
- (5) The fraction of resisting stress is neglected near the bottom of bolt where the concrete was splitted, and is neglected outside the projected circle range of $1.7 \cdot le$ radius.

The load corresponding to a given resistant stress distribution is, then, calculated as follows:

$$P = \frac{\pi \cdot f_{tx}}{\cos^2 \theta} \cdot (2 \cdot a \cdot X) - A \quad (1)$$

where, A : modification factor due to imperfect shape of stress distribution.

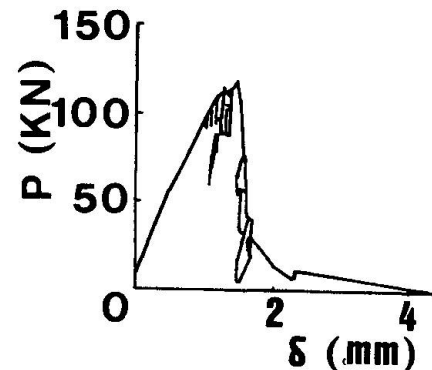


Fig.5 Load-displacement [2]

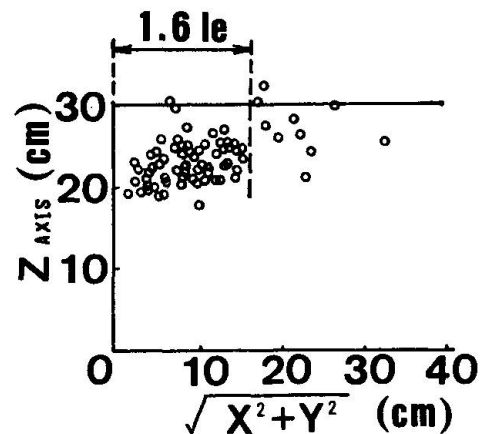


Fig.6 Acoustic emission [2]

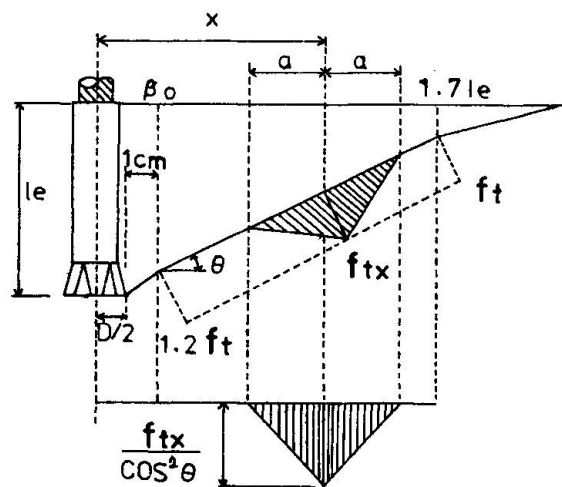


Fig.7 Proposed load carrying mechanism

The ultimate capacity of fixings is, then, calculated so as to find the maximum value of P in Eq.(1) in the supposed failure surface. In addition, the resistant stress conditions could be correlated to the load-displacement curve in Fig.8. For example, at stage 1, the deformation is mainly attributed to the elastic deflection of bolt. During stages 2 through 3, crack propagates at an angle of θ and the cracked portion of concrete is lifted up. The displacement may be due to the flexural deflection of cracked portion.

5. COMPARISON OF CALCULATION WITH TEST

5.1 In general

For calculation by the model, it is necessary to determine the angle of θ and the base length (a) of the shape of stress distribution in advance. In this study the angle of θ was fixed as 27 degree which was the mean value of the experimental results. On the contrary, there was not any rational method to determine the length (a) at this moment. Then, the length (a) was chosen as 2.7 cm which was the best fit value to the test results after several trial and error calculations. Fig.9 shows the comparison of calculated results with test results having the factor of correlation of 97.5 %.

5.2 Near Edge

The model with the same values of θ and (a) was applied to the case in which the bolts were mounted near the edge of concrete block. The resistant stress outside the edge was naturally neglected as shown in Fig.10. The comparison is shown in Fig.11. which was slightly less than that of general cases. This may be attributed to (1) the less confinement effect near the edge of concrete block, and (2) the difference of the failure pattern from the assumed one. However, the value of 91.9 % might not be so bad in prediction.

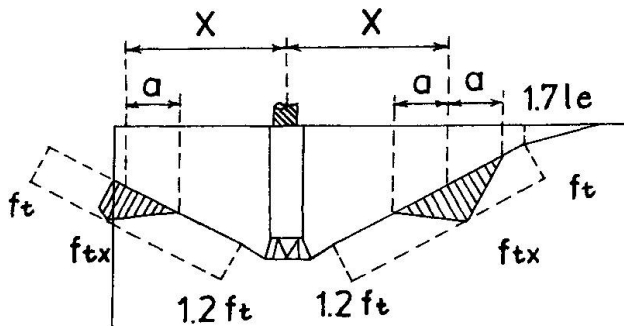


Fig.10 Stress distribution near edge

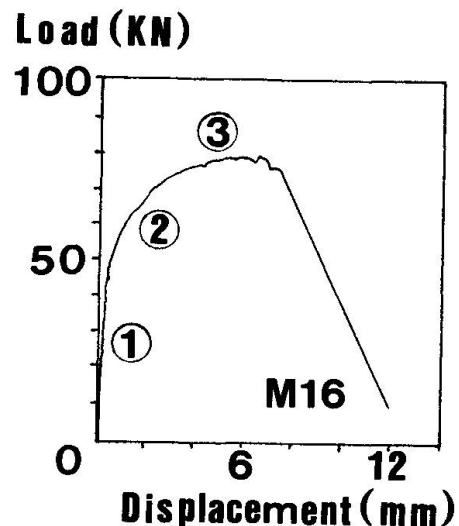


Fig.8 Load-displacement

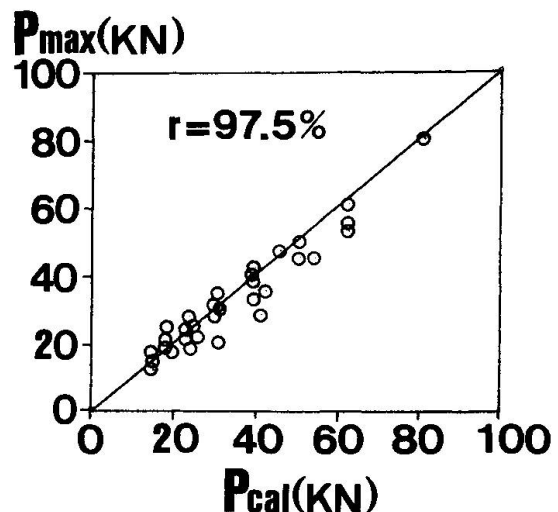


Fig.9 Comparison with test

The factor of correlation was 91.9 % which was slightly less than that of general cases. This may be attributed to

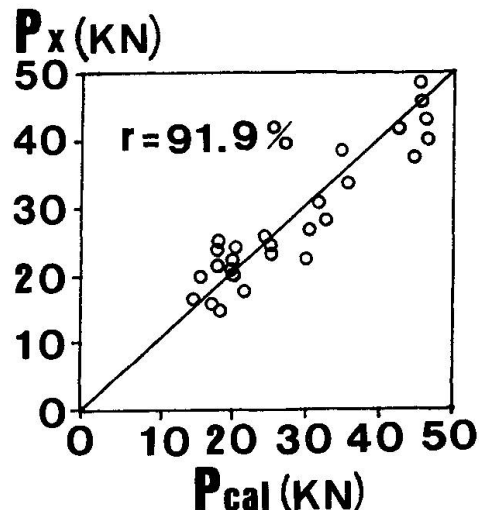


Fig.11 Comparison with test



6. FATIGUE CAPACITY OF FIXINGS

Varying the applied cyclic load level, the fatigue life of fixings was examined. The test results are plotted in Fig.12, where the solid circles represent the cases of bolt fracture and the open circles are those of concrete rupture in a conical shape. The solid line is drawn from the equation for the fatigue life of bolt (Eq.2), and the broken lines are from the equation for concrete (Eq.3). Both equations are proposed by the Japan Society of Civil Engineers [6].

$$f_{srd} = 1900 \cdot (10^{\alpha/N^k}) \cdot (1 - \sigma_{sp}/f_{ud}) \quad (2)$$

where, $\alpha = 0.82 - 0.003\phi$, $k = 0.12$,
 ϕ = diameter of bolt (mm).

$$\log N = 17 \cdot \{1 - (\sigma_{max} - \sigma_{min}) / (f_u - \sigma_{min})\} \quad (3)$$

where, σ_{max} = maximum stress in concrete due to the model, σ_{min} = minimum stress and f_u = static strength.

7. CONCLUSIONS

The followings were concluded from this study.

- (1) The resistance of concrete against the pull-out force of bolt may be attributed to the area within the projected circle with a radius of 1.7 times of the embedment length of bolt.
- (2) The pull-out resistant capacity of the fixings can be predicted by the proposed model. The model is also applicable to the fixings used near the edge of concrete structures.

REFERENCE

- [1] MARUYAMA, K., MOMOSE, M. and SHIMIZU, K., Mechanical Behavior of Undercut Type Fixings. Transactions of the JCI, Vol.11, 1989, pp.531-538.
- [2] ROKUGO, K. and et al, Pull-out test of anchor bolts and examination of failure processing by means of acoustic emission. Proceedings of the JSCE 43rd annual meeting, Part 5, 1988, pp.418-419. (in Japanese)
- [3] KAMIMURA, K. and et al, Influence of Concrete Properties upon Pull-out Strength of Mechanical Anchor Embedded in Concrete Members. Proceedings of JCI, Vol.8, 1986, pp.405-408. (in Japanese)
- [4] KOSAKA, Y. and et al, Effects of Various Factors on Pull-out Strength of Hole-in Anchors Embedded into Hardened Concrete. Proceedings of CAJ 36th General Meeting, 1982, pp.195-198. (in Japanese)
- [5] OHTANI, Y. and et al, Failure mechanism of stud anchor in tension. Proceedings of the JSCE 43rd annual meeting, Part 1, 1988, pp.372-373. (in Japanese)
- [6] JAPAN SOCIETY OF CIVIL ENGINEERS, Standard Specification for Design and Construction of Concrete Structures - 1986, Part I (Design). 1986, p.244.

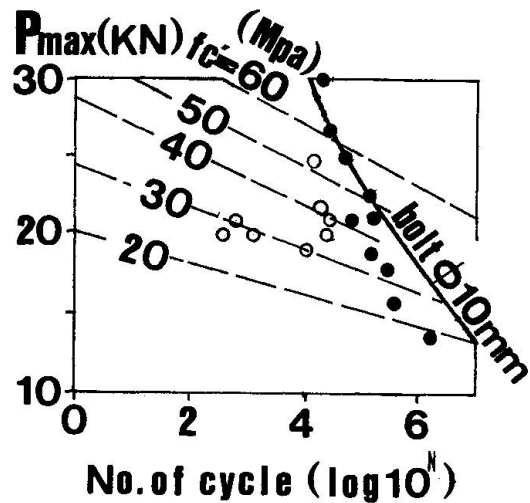


Fig.12 Fatigue Capacity